**MINERALOGY OF INTERCRATER AND INTRACRATER PLAINS IN TYRRHENA TERRA, MARS: A CASE STUDY** A. R. Boyd[1,2], K. D. Seelos[2], F. P. Seelos[2], [1]University of Maryland, College Park, 3420D SCC 3, 4318 Knox Road, College Park, MD 20742 (aroyab@terpmail.umd.edu), [2]JHU Applied Physics Laboratory, Laurel, MD 20723.

**Introduction:** In the Noachian cratered highlands of Mars, lower elevation areas often contain smoother, superposed plains deposits. These may be intercrater (between craters) or intracrater (inside craters) deposits. The heavily cratered and fluvially dissected highland terrain is generally composed of mafic to ultramafic materials with localized secondary mineral outcrops of phyllosilicates, carbonates, and salts [e.g., 1]; however, the unaltered mafic properties of the plains deposits are distinct [2]. Typically, both intercrater and intracrater plains exhibit elevated thermal inertia values and enhanced olivine and pyroxene spectral signatures [3, 4, 5]. Despite their similarities, it is unclear whether the intracrater and intercrater plains share the same emplacement mechanism. Previous studies suggest a variety of origins, including volcanic [6], from decompression melting [7] (inside craters), or lacustrine [8].

This project examines an unusual conjoined intra- and inter-crater plains feature that might give insight into the formation of similar Noachian deposits elsewhere. Located in the northwest rim region of Hellas Basin (centered approximately -24.7° N, 59° E), the crater of interest is filled with smooth plains that appear to breach the rim and extend to the southwest. The surrounding area is heavily eroded with channels, knobs/montes, and craters. Here, we build upon previous morphologic mapping [9] to examine the mineralogy of these materials to give insight into the plains' formation mechanism(s).

**Datasets and Methodology:** Mineralogic characteristics were determined using 180 m/pixel multispectral mapping and 20 m/pix targeted data from the Compact Reconnaissance Imaging Spectrometer for Mars (CRISM) [10]. CRISM summary parameters that quantify the presence of spectral features are rendered in colorized single band or 3-color (RGB) composites (Fig. 2). The 100 m/pixel thermal inertia controlled mosaics from the Thermal Emission Imaging System (THEMIS) [11] and High Resolution Stereo Camera (HRSC) [12] datasets provided contextual information. Maps were overlaid on the 100 m/pixel daytime controlled mosaic from THEMIS and 6 m/pixel broadband visible data from the Context Camera (CTX) [13]. Spatial units were delineated using JMARS [14] and only where CRISM mapping data exist.

**Mineralogy: Figure 1** gives an overview of the mineralogy of the study area, while **Figure 2** highlights contributing datasets. The plains material corresponds to the prominent Olivine, HCP (high-calcium pyroxene) unit centered in the scene, with smaller occurrences distributed throughout the study area. Other olivine-bearing terrains, LCP (low-calcium pyroxene), and phyllosilicate-bearing units are associated with knobby or cratered landforms, which is typical of the larger region [e.g., 1].

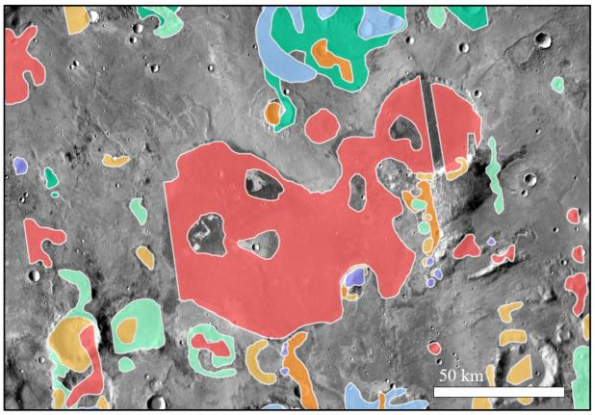


***Figure 1.*** *Color-coded mineralogic map of the study region over THEMIS daytime IR.*

| | | | |
|---|---|---|---|
| | Fe/Mg phyllosilicates | | Fe-olivine, plagioclase |
| | Prehenite, chlorite epidote, Ca/Fe carbonate | | Crystalline Fe2+ silicates |
| | Olivine, crystalline Fe2+, Fe-phyllosilicate | | Olivine, HCP |
| | LCP | | |

***Table 1:*** *Map legend.*

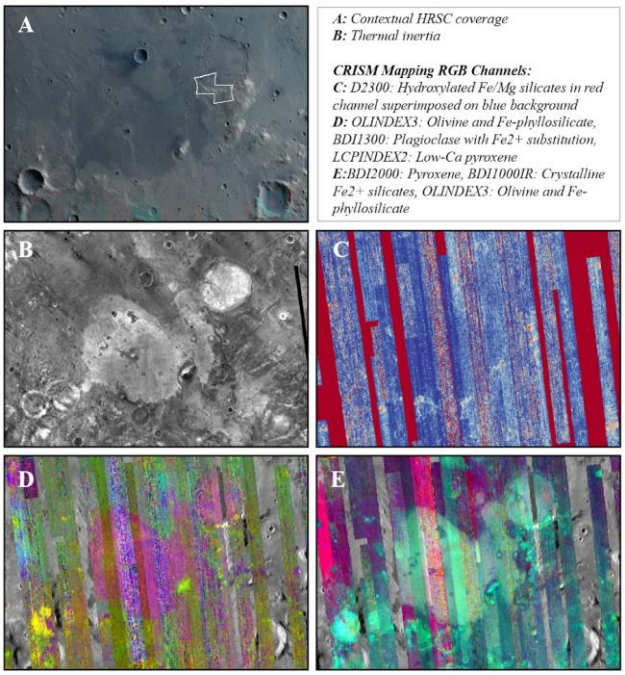


***Figure 2.*** *Contextual imaging and CRISM summary parameter composites used to delineate mineralogic units. Outline for Figure 3 is shown in (A).*

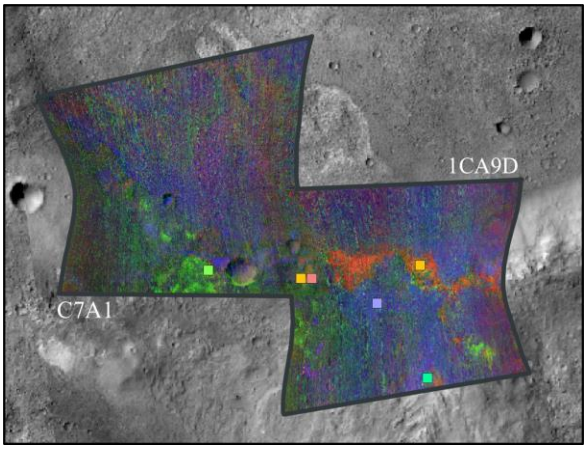


***Figure 3.*** *CRISM targeted observation mosaic, highlighting olivine, hydroxylated Fe/Mg silicates, and low-Ca pyroxene (RGB: OLINDEX3, D2300, LCPINDEX2) in the study area. Corresponding image footprints are found in* ***Fig. 2A.***

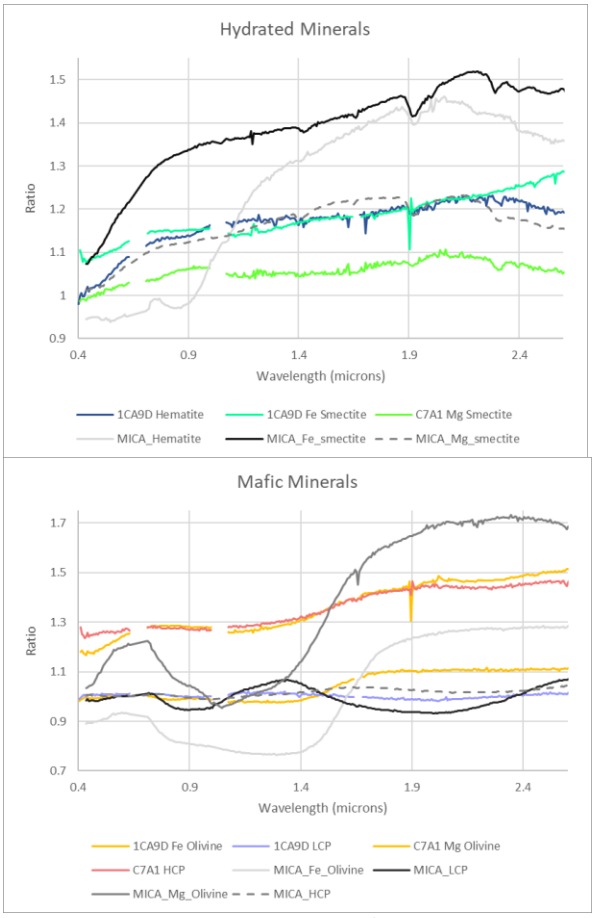


***Figure 4.*** *Ratio spectra derived from CRISM targeted observations (Fig. 3) for (A) hydrated minerals (e.g., phyllosilicates) and (B) mafic minerals (e.g., olivine and pyroxene). Scene spectra are compared to CRISM MICA library spectra [15]. Locations of spectra are indicated, by color, in* ***Fig. 3.***

CRISM targeted observations located along the boundary between the crater rim hosting the superposed intracrater plains (**Fig. 2A, 3**) confirm the presence of these minerals. Spectra indicate the presence of Fe-olivine, LCP, and Fe/Mg smectite in the crater rim while more HCP- and Mg-olivine bearing materials are associated with the plains. The alignment of diagnostic absorption features between CRISM reference (MICA) spectra and extracted scene spectra validates the presence of the dominant minerals identified using the multispectral data (**Fig. 1**).

**Conclusion:** Previous morphologic mapping [9] of the study area combined with mineralogic information presented here suggest that the intracrater and intercrater plains were emplaced through the same mechanism, which is most likely volcanic activity. Future work will more closely examine the stratigraphic and relative age relationships of the mapped units and also expand our comparison to similar exposures in the larger Tyrrhena Terra region.

**Acknowledgments:** Data used in this study are publicly available from the NASA Planetary Data System (PDS) and were accessed and examined using ASU/JMARS. The research was funded by the Mars Data Analysis Program (MDAP) and the MRO/CRISM project.

**References:** [1] Ehlmann B. L. and Edwards C. S. (2014) *Ann. Rev. of Earth and Plan. Sci.*, *42*, 291-315. [2] Rogers A. D. and Nazarian A. H. (2013) *JGR*, *118*, 1094–1113. [3] Rogers D. A. and Hamilton V. E. (2014) *JGR*, *120*, 69-91. [4] Koeppen W. C. and Hamilton V. E. (2008) *JGR*, *113(E5)*, E05001. [5] Mustard J. F. et al. (2005) *Science*, *307*, 1594–1597. [6] Head J. W. et al. (2006) *Geology*, *34*, 285. [7] Edwards C. S. et al. (2014) *Icarus*, *228*, 149–166. [8] Goudge T. A. et al. (2012) *JGR*, *117*, E00J2. [9] Boyd A. R. et al. (2022) *LPSC LIII*, Abstract #2769. [10] Murchie S. et al. (2007) *Geophys. Res. Planets*, *112*. [11] Fergason R. L. et al. (2013) *LPSC XLIV*, Abstract #1642. [12] Neukum G. et al. (2009) *Mars Express: The Scientific Investigations*, 15-74. [13] Malin M. C. et al. (2007) JGR, 112, E05S04. [14] Christensen P. R. et al. (2009) *American Geophysical Union*, Abstract #IN22A-06. [15] Viviano-Beck et al. (2014) *JGR*, 119, 1403– 1431.